

# A Prospective Study to Assess In Vivo Optical Coherence Tomography Imaging for Early Detection of Chemotherapy-Induced Oral Mucositis

Alden Calantog, BS,<sup>1</sup> Lucy Hallajian, BS,<sup>1</sup> Tasneem Nabelsi, BS,<sup>1</sup> Stephanie Mansour, BS,<sup>1</sup> Anh Le, DDS, PhD,<sup>2</sup> Joel Epstein, DMD, MSD, FRCD(C) FDS RCS(Edin),<sup>3</sup> and Petra Wilder-Smith, DDS, PhD<sup>1\*</sup>

<sup>1</sup>Beckman Laser Institute, University of California, Irvine, California 92612

<sup>2</sup>Department of Oral and Maxillofacial Surgery/Pharmacology, University of Pennsylvania, 240 South 40th Street, Philadelphia, Pennsylvania 19104

<sup>3</sup>Division of Otolaryngology and Head and Neck Surgery, City of Hope 1500 East Duarte Road, Duarte, California 91010

**Background and Objective:** Oral mucositis (OM) is a common and severe complication of many cancer therapies. Currently, prediction and early detection are not possible and objective monitoring remains problematic. Goal of this prospective study is to assess non-invasive imaging using optical coherence tomography (OCT) for early detection and evaluation of chemotherapy-induced OM in 48 patients, 12 of whom developed clinical mucositis.

**Study Design/Materials and Methods:** In 48 patients receiving neoadjuvant chemotherapy for primary breast cancer, oral mucosal health was assessed clinically, and imaged using non-invasive OCT. Images were evaluated for mucositis using an imaging-based scoring system ranging from 0 to 6. Conventional clinical assessment using the OM assessment scale (OMAS) was used as the gold standard. Patients were evaluated on Days 0–11 after commencement of chemotherapy. OCT images were visually scored by three blinded investigators.

**Results:** The following events were identified from OCT images (1) change in epithelial thickness and subepithelial tissue integrity (beginning on Day 2), (2) loss of surface keratinized layer continuity (beginning on Day 4), (3) loss of epithelial integrity (beginning on Day 4). Imaging data gave higher scores compared to clinical scores early in treatment, suggesting that the imaging-based diagnostic scoring was more sensitive to early mucositis change than the clinical scoring system. Once mucositis was established, imaging and clinical scores converged.

**Conclusion:** Using OCT imaging and a novel scoring system, earlier, more sensitive detection of mucositis was possible than using OMAS. Specific imaging-based changes were a consistent predictor of clinical mucositis. *Lasers Surg. Med.* 45:22–27, 2013.

© 2013 Wiley Periodicals, Inc.

**Key words:** cancer therapy; imaging; monitoring; oral diagnosis; oral mucosa; prediction

## INTRODUCTION

### Oropharyngeal Mucositis

Oropharyngeal mucositis (OM) occurs in up to 75% of chemotherapy patients or those receiving hematopoietic cell transplant (HCT), and in essentially all patients receiving head and neck radiation in doses over 5,000 cGy. Ulcerative mucositis is the most common cause of severe pain in HCT and treatments for hematologic cancer. While advances in HCT have led to a modest reduction in the frequency of severe oral ulcerative mucositis, changes in treatment of head and neck cancer including combined chemotherapy and irradiation as well as changes in radiation therapy dosing schedules have increased the severity and duration of mucositis in these patients [1].

OM may lead to alterations in cancer therapy, dose reduction, delay in scheduled therapy, and may require interruption or termination of planned therapy, with the potential for impact on patient cure. In addition, OM is associated with a negative impact on quality of life (QOL) and increases cost of care [2–5]. OM is the most common distressing and disabling acute complication of cancer chemotherapy [6] and radiotherapy [7] as reported by patients, and is among the most significant major dose-limiting toxicities of cancer therapy [8–10].

**Conflict of Interest Disclosures:** All authors have completed and submitted the ICMJE Form for Disclosure of Potential Conflicts of Interest and none were reported.

Contract grant sponsor: NIH (NIBIB); Contract grant number: R03 DB014852; Contract grant sponsor: NIH (NIBIB); Contract grant number: P41EB015890.

\*Corresponding to: Petra Wilder-Smith, DDS, PhD, Associate Professor and Director of Dentistry, Beckman Laser Institute, University of California at Irvine, 1002 Health Sciences Rd. East, Irvine, CA 92612. E-mail: pwsmith@uci.edu

Accepted 12 December 2012

Published online 15 January 2013 in Wiley Online Library (wileyonlinelibrary.com).

DOI 10.1002/lsm.22111

### Existing techniques for predicting and characterizing OM

Clinically, OM [10] is characterized by mucosal changes, including erythema and ulceration, which cause oropharyngeal pain. Currently, prediction of onset and severity of mucositis is not possible, and early detection is not feasible, as the condition is diagnosed and classified by its clinical manifestations. This inability hampers efforts at early, targeted intervention and affects overall treatment effectiveness. Precise evaluation of lesions induced by specific treatment regimens and accurate monitoring of the effects of interventions for OM is not possible. Moreover, our understanding of the pathogenesis of mucositis would be greatly enhanced by the ability to detect early, monitor and characterize OM *in vivo* and non-invasively.

### Optical Coherence Tomography

Optical coherence tomography (OCT) is an emerging non-invasive, high resolution optical imaging modality that uses near-infrared light instead of ionizing radiation to provide high-resolution sub-surface tissue images [11–13]. Conceptually, it is in many ways comparable to ultrasound scanning, except that light is used instead of sound [13]. Broadband laser light waves are emitted from a source and directed toward a beam splitter, one wave is sent toward a reference mirror with known path length and the other toward the tissue sample. After the two beams reflect off the reference mirror and tissue sample surfaces at varying depths within the sample, the reflected light is directed back towards the beam splitter, where the waves are recombined and read with a photo detector. The image is produced by analyzing interference of the recombined light waves. Cross-sectional images of tissues are constructed in real time, at near histological resolution (approximately 10  $\mu\text{m}$  with current technology). With the latest technologies, 3D volume scans that can be manipulated tomographically to produce 2D pull-out images in specific sites of interest have become possible [14]. This permits *in vivo* non-invasive imaging of the microscopic characteristics of epithelial and subepithelial structures.

With a tissue penetration depth of approximately 2 mm, the OCT technology described in this paper is suitable for imaging of the oral mucosa [14–22]. Compact, mobile, user-friendly clinical OCT systems are now becoming available to clinicians, offering small, flexible fiberoptic OCT probes that can easily access the oral cavity to provide chair side *in vivo* clinical imaging, and immediate, real-time OCT images, with total imaging times per scan of usually a second or less. Digital data files provide quick and easy data storage, retrieval, and printouts as needed.

Previous studies using OCT have demonstrated the ability to evaluate characteristics of epithelial, subepithelial, and basement membrane structures and show the potential for near histopathological-level resolution and close correlation with histological appearance [14–22]. Two studies have reported the successful use of OCT for

the early detection and quantification of radiation- and chemotherapy-induced mucositis in the mouse and hamster models [23,24], with one paper [24] reporting the validation of an imaging-based scale as a means of detecting mucositis change earlier than the clinical OMAS scale, and with convergence between the two scales after a few days. A similar, somewhat simpler scale underwent preliminary testing in five subjects with comparable results, demonstrating the potential of OCT imaging for diagnosing the onset of mucositis typically 2–3 days prior to the development of any clinical symptoms [25].

In this study, (1) the ability of OCT to *predict* chemotherapy-induced oral mucositis (OM), (2) the ability of OCT to *detect* mucositis, and (3) the *usefulness* of an imaging-based diagnostic scale versus, the current gold standard, the OMAS scale, were evaluated in 48 human subjects.

## MATERIALS AND METHODS

### Human Subjects, Clinical, and Imaging Procedure

Forty-eight female human subjects receiving neoadjuvant chemotherapy for primary breast cancer were consented and enrolled in this study as approved under UCI IRB approval 2002–2805. Five of these patients had undergone previous cycles of chemotherapy and had developed mucositis during that treatment phase. The likelihood of developing mucositis is high in patients who have suffered from mucositis during the previous cycle of chemotherapy. The remaining 43 patients were due to begin their first cycle of chemotherapy at the time when they were enrolled in this study. Informed written consent was obtained from all patients. After enrollment in this study, a full oral examination was completed, and baseline photographs of the healthy oral mucosa were taken in the following areas: left and right cheek, dorsal and ventral surface of the tongue, lateral borders of the tongue, upper and lower labial sulci, buccal/labial gingivae. Photographs were immediately printed out, and the scan line locations for the baseline OCT imaging conducted at that time were marked on the photographs. Imaging was performed using a hand-held fiber-optic probe and 6 mm scan lines. Each location was scanned three times to assess the reproducibility of the images obtained. This procedure was repeated on Days 2, 4, 7, and 11 after the commencement of chemotherapy. These imaging time points were dictated by patient availability. Ideally the patients would have been imaged daily, especially in the early days immediately after commencement of chemotherapy.

### Clinical Scoring of Mucositis: OMAS scale

Clinical evaluation was documented at each time-point directly in patients using the standard oral mucositis assessment scale (OMAS; by three observers, PWS, AC, and LH) to assess erythema and ulceration in oral tissue (Tables 1 and 2), combined with a visual analog pain scale (VAS). OMAS was developed by a working group, and validated as published in *Cancer* [2,5]. It is a cumulative scoring system on a scale of 0–5, which has been shown to be highly reproducible between observers ( $r > 0.8$ ),

**TABLE 1. Cumulative Scoring System in a Scale of 0–5 for Clinical Evaluation of Mucositis Based on OMAS Scale**

Ulcer	Redness		
	0	1	2
0	0	1	2
1	1	2	3
2	2	3	4
3	3	4	5

responsive over time ( $r > 0.9$ ) and it accurately records the anatomic elements considered to be associated with mucositis. This scoring tool has since been employed in several multicenter mucositis studies [2,3,6–10].

**Optical Coherence Tomography (OCT)**

All subjects were imaged using the same commercially available Niris<sup>®</sup> OCT console and imaging probe (Imalux Corporation, Cleveland, OH), which allows real-time video rate imaging speed, simultaneous OCT and CCD imaging channels, 3D volumetric imaging and surface profiling capability at an imaging depth of up to 50  $\mu\text{m}$ . The imaging system has approximately 8–15  $\mu\text{m}$  depth resolution and 20  $\mu\text{m}$  lateral resolution.

**Evaluation of OCT Data**

A semi-quantitative OCT scale for scoring mucositis was used as previously described [25] and depicted in Table 3. This scale has a total scoring range of 0–6, with six corresponding to the most severe condition. OCT images were coded to blind the evaluators (PWS, SD, TL) to their source. Scorers had been pre-standardized to 96% accuracy using an existing database of OCT images as previously described [25]. All images were scored in one session and evaluated for changes in epithelial thickness, loss of surface integrity, and loss of subsurface integrity. The individual scores from the three scorers were then combined to generate one cumulative final score. Where

**TABLE 2. OMAS Scale for Oral Mucositis**

Location	Ulceration-a	Erythema-b
Lip—upper	0, 1, 2, or 3	0, 1, or 2
Lip—lower	0, 1, 2, or 3	0, 1, or 2
Buccal mucosa—right	0, 1, 2, or 3	0, 1, or 2
Buccal mucosa—left	0, 1, 2, or 3	0, 1, or 2
Tongue ventrolateral—right	0, 1, 2, or 3	0, 1, or 2
Tongue ventrolateral—left	0, 1, 2, or 3	0, 1, or 2
Floor of mouth	0, 1, 2, or 3	0, 1, or 2
Palate—soft	0, 1, 2, or 3	0, 1, or 2
Palate—hard	0, 1, 2, or 3	0, 1, or 2

(a) Area of ulceration: 0 = none,  $1 \leq 1 \text{ cm}^2$ ,  $2 = 1\text{--}3 \text{ cm}^2$ ,  $3 \geq 3 \text{ cm}^2$ .

(b) severity of erythema: 0 = none, 1 = not severe, 2 = severe.

**TABLE 3. OCT-Based Scale for Assessing Oral Mucositis**

Scoring of OCT-visible mucositis changes	
A. Epithelial thickness	
Score 0:	same as Day 0 ( $\pm 20\%$ )
Score 1:	reduced versus Day 0 by $<50\%$
Score 2:	Reduced versus Day 0 by 50–99%
Score 3:	Reduced versus Day 0 by $>99\%$
B. Loss of surface integrity	
Score 1	if yes
C. Loss of subsurface integrity	
Score 2	if yes
Thus, total scoring range for OCT (structural) lies between 0 and 6	

several diagnostic scores for any attribute in one lesion were possible, the most severe score was used.

**RESULTS**

**Clinical Data**

Twelve of the 48 patients developed clinical mucositis, which was defined as an OMAS score  $>1$ . Mucositic severity ranged from low-grade to high-grade. Changes evident in the oral mucosa following chemotherapy included the following: no clinical changes, mucosal erythema, micro-ulceration, frank open ulceration, surface necrosis and sloughing, mucosal breakdown and healing.

Figures 1 and 2 show mean OMAS score (SE) over time for the patients included in this study. Based on their

**OMAS vs. Imaging Score in patients who developed clinical mucositis**

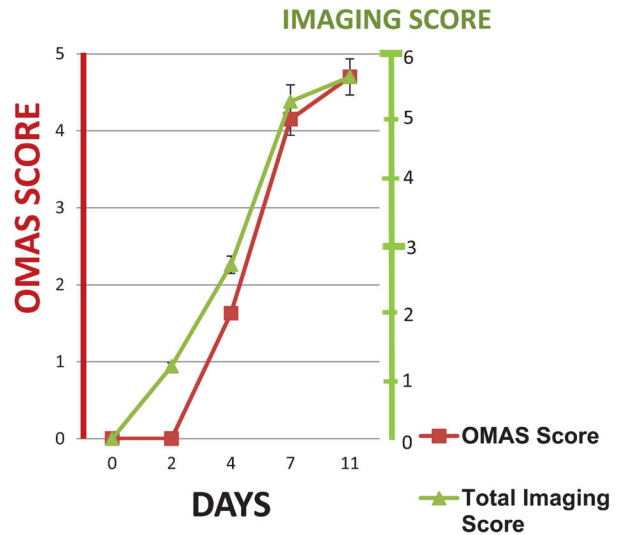


Fig. 1. Mean (SE) OMAS versus imaging score over time in patients who developed clinical mucositis (OMAS  $> 1$ ). OMAS scale axis on LHS; Imaging score axis on RHS.

### OMAS vs Imaging Score in patients who did not develop clinical mucositis

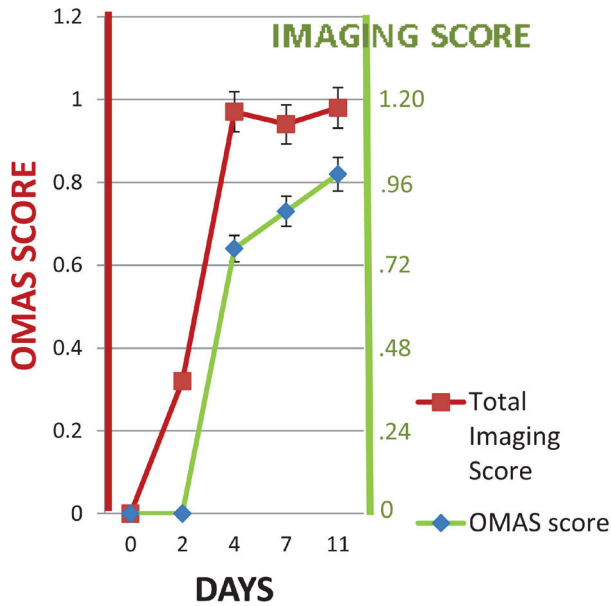


Fig. 2. Mean (SE) OMAS versus imaging score over time in patients who did not develop clinical mucositis (OMAS < 1).

response to chemotherapy, subjects were divided into two groups for the purposes of data analysis. Subjects in Group 1 developed clinical signs of mucositis, with an OMAS score that exceeded 1 at one or more time points during the duration of the study. For the “no clinical mucositis” patients allocated to Group 2, OMAS scores consistently remained below or at 1 throughout the duration of the study.

#### Imaging Data

OCT imaging was rapid and simple, with an average imaging time of <1 minute per site. Movement artifacts during OCT registration were successfully avoided by seating subjects in a chair with headrest and neck support.

In the OCT images, stratified squamous epithelium is visible, separated from the lamina propria (LP) by the basement membrane. The darker appearance of the epithelium is related to its lower optical density and scattering properties, which result in lower signal intensity. The LP is a more optically dense tissue and appears brighter due to higher signal intensity (Fig. 3). In some images the surface appears particularly bright because in many sites it is overlapped by the bright reflection from the cover of the imaging probe (P). When blood vessels are visible, an “optical shadow” causing image loss beyond the point of the proximal vessel lumen is sometimes seen. This is due to light absorption by hemoglobin.

**Comparison of Clinical Mucositis Scores (OMAS) Versus Imaging Scores.** Using imaging, the following

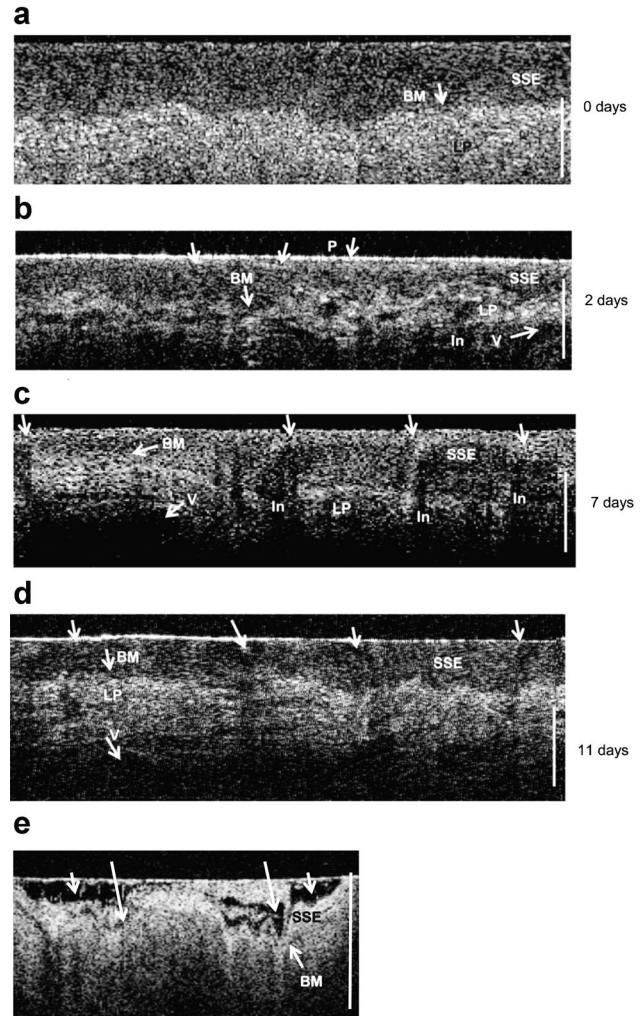


Fig. 3. In vivo OCT images of buccal surface of cheek before (a), after 2 days (b), after 7 days (c), and after 11 days (d, e) of chemotherapy. Vertical bar is 500  $\mu$ m. In (a), stratified squamous epithelium (SSE) is visible, separated from the lamina propria (LP) by the basement membrane (BM). Tissues all appear normal and OCT imaging score is 0. After 2 days (b), epithelium is thinner by 30–40%, surface is still intact, although directly below the surface some breakdown is apparent (arrow). The surface appears bright and intact because it in many sites is overlapped by the bright reflection from the cover of the imaging probe (P). Subepithelial tissues just below the basement membrane show considerable disruption. An engorged blood vessel is visible (V). At this point, the patient was totally asymptomatic. OCT imaging score is 3. Further epithelial atrophy is seen after 7, 11 days (c, d), with infiltrate (In) around the basement membrane and disruption of the adjacent epithelial and subepithelial tissues (arrows), and breakdown of the epithelial surface (arrows). OCT imaging score for C is 4 and for D is 5.

events were detected: (1) change in epithelial thickness and loss of subepithelial integrity (Day 2 onwards), (2) loss of surface keratinized layer continuity (Day 4 onwards), (3) loss of epithelial integrity (Day 7 onwards). Figure 1 shows the OCT imaging score (and SE) and OMAS score during the development of mucositis. In the 12 patients who developed clinical mucositis, the condition was consistently detected earlier by OCT than using OMAS. This was true regardless of the level of clinical mucositis that ensued. Nine patients showed signs of mucositis on Day 2 using the OCT-based imaging scale. These patients all developed first signs of clinical mucositis by Day 4 or 7. By Day 4, the remaining three patients showed mucositis based on the imaging data, but no clinical signs of the condition. All of these patients exhibited clinical mucositis by Day 7 or 11.

In a typical patient whose OMAS score was 0 on Day 2, and who developed OMAS Grade 1 mucositis on Day 4 and OMAS Grade 2 on Day 8, the OCT image from Day 2 already demonstrated mucositic change (Fig. 3). Features visible in the OCT image include epithelial thinning by an average of 40% and disruption of the subepithelial layers just below the basement membrane, resulting in an OCT imaging score of 2. An enlarged blood vessel is also visible. Further epithelial atrophy is seen on Days 7 and 11 after chemotherapy with infiltrate in the area of the basement membrane, disruption of the adjacent epithelial and subepithelial tissues, and breakdown of the epithelial surface. Subepithelial liquefaction degeneration and a greatly engorged blood vessel are also visible. The somewhat reduced imaging capability of OCT on Days 7 and 11 in the deeper tissues may be due to hyperemia in the tissues. Light at 1,300 nm is strongly absorbed by blood, mainly due to its water content. Thus mucositic change was detected earlier using OCT imaging than by conventional clinical examination, and predicted changes were observed several days later in the visual clinical examination.

In the patients who developed clinical mucositis, differences in the OCT imaging score between each pair of successive time points were significant with  $P < 0.05$  using the Kruskal–Wallis nonparametric test, which is appropriate given the relatively small numbers. This means that the OCT imaging score was capable of mapping the changes in the severity of the mucositic condition that developed between assessment visits. The OCT imaging score tended to give higher scores compared to clinical scores early on (Days 0–4). However correspondence was good at Days 7 and 11 (non-significant Wilcoxon rank-sum test and moderate Spearman and Pearson correlation coefficients). These data indicate that the OCT imaging score was more sensitive to early mucositic change than the clinical scoring system. Clinically, this finding is important, as earlier detection of mucositic change will allow the earlier and more effective instigation of anti-mucositic measures. Once mucositis was established and the clinical manifestation of the condition was more advanced, the imaging and clinical scores converged.

In the subjects that did not develop clinical mucositis, the imaging score did not change significantly ( $P < 0.05$ )

between Day 0 (Score 0) and Day 2 (Score 0.15; Fig. 2). However, by Day 4 the imaging score had increased significantly ( $P < 0.05$ ) in 27 of the subjects with a mean value of 0.46, demonstrating a subclinical mucositic response and it remained at a similar level throughout the duration of the study.

## DISCUSSION

For many years, mucositis was thought to result from negative effects by cancer therapies on epithelial cell replication. However, the development of animal models and more refined cellular biology techniques in research has resulted in the identification of a complex pathobiology of mucositis. It is now clear that a multitude of molecular events is initiated, and that it is the submucosa rather than the oral epithelial surface that is primarily targeted by these events [26,27]. This finding was described in pilot *in vivo* imaging studies [23–25] and confirmed in this study. In all four investigations, subepithelial damage was apparent prior to the onset of any epithelial changes in the hamster model and in human subjects receiving cancer therapy. According to Sonis [26,27], radiation therapy or chemotherapy directly injures DNA by generation of reactive oxygen species and stimulation of transcription factors, resulting in death in a few of the cells during the first or initiation phase of mucositis (Days 0–2). In Phase 2 (Days 2–3), inflammatory cytokines are released, causing further tissue injury, cell death, and mucosal thinning. Angiogenesis and fibroblast breakdown also occur. Erythema may begin to develop. In this imaging study, epithelial thickness was reduced by 25–70% by Day 4 in subjects who later developed clinical mucositis, and by 10–40% in subjects who did not later develop clinical mucositis. During Phase 3 (Days 2–10), direct damage to cells and escalation of the process results from signaling and amplification of the process initiated by proinflammatory cytokines. At this stage, most of the damage occurs submucosally. In this study, disruption of the epithelial and subepithelial layers just below the basement membrane was clearly visible at this time point in 11 of the 12 subjects who developed clinical mucositis. Feldchtein et al. and Wilder-Smith et al. reported similar findings using *in vivo* imaging in animals and humans [23–25].

Clinical ulceration extending from epithelium to submucosa typically is seen in Phase 4. This can be accompanied by pseudomembrane formation, bacterial colonization, and further stimulation of proinflammatory cytokines. Severe pain is caused by mucosal damage and the exposure of nerve endings. At this stage, imaging is no longer necessary to detect and observe mucositis. Interestingly, the OCT images show a remarkably deep level of tissue disruption underneath some of the ulcers (Fig. 3d and e). In Phase 5, healing begins, with adjacent epithelial cells migrating into the ulcers and proliferating to re-form the normal stratifications of the oral mucosa. The oral microflora also begins to regenerate. However, cells underneath the epithelial surface never recover fully, leaving the patient susceptible to future damage.

These preliminary studies demonstrate the potential of non-invasive OCT imaging for assessing oral cancer therapy-induced mucositis. More comprehensive studies are now underway to define diagnostic cut-off points for the imaging markers to maximize diagnostic sensitivity, specificity, and predictive values.

### Conclusion

These preliminary studies demonstrate the potential of non-invasive OCT imaging for detecting and semi-quantifying oral cancer therapy-induced mucositis. Moreover, clinical mucositis was always preceded by subsurface mucosal changes that were readily apparent in OCT images. More extensive studies are in progress that will permit the closer delineation of imaging markers and their diagnostic cut-off points and also provide a more comprehensive evaluation and statistical analysis of this modality.

### ACKNOWLEDGMENTS

We gratefully acknowledge the following funding support: NIH (NIBIB) R03 DB014852; NIH (NIBIB) P41EB015890.

### REFERENCES

1. Modi BJ, Knab B, Feldman LE, Mundt AJ, Yao M, Pytynia KB, Epstein J. Review of current treatment practices for carcinoma of the head and neck. *Exp Opin Pharmacother* 2005;6:1143–1155.
2. Sonis ST, Elting LS, Keefe D, Peterson DE, Schubert M, Hauer-Jensen M, Rubenstein EB. Perspectives on cancer therapy-induced mucosal injury: Pathogenesis, measurement, epidemiology, and consequences for patients. *Cancer* 2004;100:1995–2025.
3. Sonis ST, Oster G, Fuchs H, Bellm L, Williamson BZ, Edelsberg J, Peterson DE, Schubert MM, Spijkervet FK, Horowitz M. Oral mucositis and the clinical and economic outcomes of hematopoietic stem-cell transplantation. *J Clin Oncol* 2001;19:2201–2205.
4. Elting LS, Shih YC. The economic burden of supportive care of cancer patients. *Support Care Cancer* 2004;12:219–226.
5. Elting LS, Cooksley C, Caambers M, Cantor SBN, Manzullo F, Rubenstein EB. The burdens of cancer therapy. Clinical and economic outcomes of chemotherapy-induced mucositis. *Cancer* 2004;100:1324–1326.
6. Epstein JB, Stevenson-Moore P, Jackson SM, Mohamed JH, Spinelli JJ. Prevention of oral mucositis in radiation therapy: A controlled study with benzydamine hydrochloride rinse. *Int J Radiat Oncol Biol Phys* 1989;16:1571–1575.
7. Epstein JB. Infection prevention in bone marrow transplantation and radiation patients. *NCI Monogr* 1990;9:73–85.
8. Epstein JB, Schubert MM, Scully C. Evaluation and treatment of pain in patients with orofacial cancer: A review. *Pain Clin* 1991;4:3–20.
9. Epstein JB, Schubert M, Scully C. Evaluation and treatment of pain in patients with orofacial cancer: A review. *Pain Clin* 1991;4:3–20.
10. Epstein JB. Oral complications of cancer chemotherapy: Etiology, recognition and management. *Can J Oncol* 1992;2: 83–95.
11. Bizheva K, Unterhuber A, Hermann B, Povazay B, Sattman H, Fercher AF. Imaging ex vivo healthy and pathological human brain tissue with ultra-high-resolution optical coherence tomography. *J Biomed Opt* 2005;10:11006.
12. Brezinski ME, Fujimoto JG. Optical coherence tomography: High-resolution imaging in nontransparent tissue. *IEEE J Select Top Quantum Electron* 1999;5:1185–1192.
13. Tadrous PJ. Methods for imaging the structure and function of living tissues and cells: I. Optical coherence tomography. *J Pathol* 2000;191:115–119.
14. Jung WG, Zhang J, Wang L, Wilder-Smith P, Chen Z, McCormick DT, Tien NC. Three-dimensional optical coherence tomography employing A 2-axis MEMS. *J Biophotonics STQE* 2006;11:806.
15. Tsai MT, Lee HC, Lu CW, Wang YM, Lee CK, Yang CC, Chiang CP. Delineation of an oral cancer lesion with swept-source optical coherence tomography. *J Biomed Opt* 2008; 13(4):044012.
16. Tsai MT, Lee HC, Lee CK, Yu CH, Chen HM, Chiang CP, Chang CC, Wang YM, Yang CC. Effective indicators for diagnosis of oral cancer using optical coherence tomography. *Opt Express* 2008;16(20):15847–15862.
17. Jo JA, Applegate BE, Park J, Shrestha S, Pande P, Gimenez-Conti IB, Brandon JL. In vivo simultaneous morphological and biochemical optical imaging of oral epithelial cancer. *IEEE Trans Biomed Eng* 2010;57(10):2596–2599.
18. Jerjes W, Upile T, Conn B, Hamdoon Z, Betz CS, McKenzie G, Radhi H, Vourvachis M, El Maaytah M, Sandison A, Jay A, Hopper C. In vitro examination of suspicious oral lesions using optical coherence tomography. *Br J Oral Maxillofac Surg* 2010;48(1):18–25.
19. Wilder-Smith P, Jung WG, Brenner M, Osann K, Beydoun H, Messadi D, Chen Z. In vivo optical coherence tomography for the diagnosis of oral malignancy preliminary studies in 50 patients. *Lasers Surg Med* 2004;35:269–275.
20. Ridgway JM, Armstrong WB, Guo S, Mahmood U, Su J, Jackson RP, Shibuya T, Crumley RL, Gu M, Chen Z, Wong BJ. In vivo optical coherence tomography of the human oral cavity and oropharynx. *Arch Otolaryngol Head Neck Surg* 2006;132(10):1074–1081.
21. Ahn YC, Chung J, Wilder-Smith P, Chen Z. Multimodality approach to optical early detection and mapping of oral neoplasia. *J Biomed Opt* 2011;16(7):076007.
22. Tsai MT, Lee CK, Lee HC, Chen HM, Chiang CP, Wang YM, Yang CC. Differentiating oral lesions in different carcinogenesis stages with optical coherence tomography. *J Biomed Opt* 2009;14(4):044028.
23. Muanza TM, Cotrim A, McAuliffe M, Sowers A, Baum B, Cook J, Feldchtein F, Amazeen P, Coleman CN, Mitchel JB. Evaluation of radiation-induced oral mucositis by optical coherence tomography. *Clin Cancer Res* 2005;11:5121–5127.
24. Wilder-Smith P, Hammer-Wilson MJ, Zhang J, Wang Q, Osann K, Chen Z, Wigdor H, Schwartz J, Epstein J. In-vivo imaging of oral mucositis in an animal model using optical coherence tomography (OCT) and optical Doppler tomography (ODT). *Clin Cancer Res* 2007;13(8):2449–2454.
25. Kawakami-Wong H, Gu S, Hammer-Wilson MJ, Epstein JB, Chen Z, Wilder-Smith P. In vivo optical coherence tomography-based scoring of oral mucositis in human subjects: A pilot study. *J Biomed Opt* 2007;12(5):051702.
26. Sonis ST. A biological approach to mucositis. *J Support Oncol* 2004;2:21–32.
27. Sonis ST. Pathobiology of mucositis. *Semin Oncol Nurs* 2004;20:11–15.